

# We are IntechOpen, the world's leading publisher of Open Access books Built by scientists, for scientists

6,900

Open access books available

186,000

International authors and editors

200M

Downloads

Our authors are among the

154

Countries delivered to

TOP 1%

most cited scientists

12.2%

Contributors from top 500 universities



WEB OF SCIENCE™

Selection of our books indexed in the Book Citation Index  
in Web of Science™ Core Collection (BKCI)

Interested in publishing with us?  
Contact [book.department@intechopen.com](mailto:book.department@intechopen.com)

Numbers displayed above are based on latest data collected.  
For more information visit [www.intechopen.com](http://www.intechopen.com)



---

# Acoustic Wave Velocity Measurement on Piezoelectric Single Crystals

---

Toshio Ogawa

Additional information is available at the end of the chapter

<http://dx.doi.org/10.5772/62711>

---

## Abstract

Sound velocities were measured in relaxor single-crystal plates and piezoelectric ceramics including lead free using an ultrasonic precision thickness gauge with high-frequency pulse generation. Estimating the difference in the sound velocities and elastic constants in the single crystals and ceramics, it was possible to evaluate effects of domain and grain boundaries on elastic constants. Existence of domain boundaries in single crystal affected the decrease in Young's modulus, rigidity, Poisson's ratio, and bulk modulus. While existence of grain boundaries affected the decrease in Young's modulus and rigidity, Poisson's ratio and bulk modulus increased. It was thought these phenomena come from domain alignment by DC poling and both the boundaries act as to absorb mechanical stress by defects due to the boundaries. In addition, the origin of piezoelectricity in single crystals is caused by low bulk modulus and Poisson's ratio, and high Young's modulus and rigidity in comparison with ceramics. On the contrary, the origin of piezoelectricity in ceramics is caused by high Poisson's ratio by high bulk modulus, and furthermore, low Young's modulus and rigidity due to domain alignment.

**Keywords:** relaxor single crystals, sound velocities, elastic constants, domain boundary, grain boundary, piezoelectric ceramics

---

## 1. Introduction

### 1.1. What are relaxor materials?

Relaxor materials are one of the ferroelectric materials and show that temperatures to realize the maximum dielectric constants shift to higher temperature, and furthermore, the maximum values decrease with increasing frequency [1]. These phenomena are called "dielectric

relaxation". The relaxors are composed of lead-containing complex perovskite structures such as  $\text{Pb}(\text{Zn}_{1/3}\text{Nb}_{2/3})\text{O}_3\text{-PbTiO}_3$  (PZNT) and  $\text{Pb}(\text{Mg}_{1/3}\text{Nb}_{2/3})\text{O}_3\text{-PbTiO}_3$  (PMNT). The applications of relaxor had been focused on materials for multilayer ceramic capacitors (MLCC) because of high dielectric constants and lower firing temperature for producing MLCC [2]. Moreover, since relaxors are composed of without  $\text{PbZrO}_3$ , which is easy to decompose at high temperatures, they were suitable to produce piezoelectric single crystals in comparison with in the case of well-known  $\text{PbTiO}_3\text{-PbZrO}_3$  (PZT) compositions [3].

## 1.2. Why do single crystals possess high performance of piezoelectricity?

Piezoelectric ceramic compositions were improved to realize higher electromechanical coupling factor from one-component system such as  $\text{BaTiO}_3$  (BT) to binary system of PZT and three-component (PZT 3) system as shown in **Figure 1** [4, 5]. Since high piezoelectricity closely relates to ferroelectric domain alignment by DC poling, a research for piezoelectric single crystals without (with no existence of) grain boundary becomes important. In 1982, Kuwata et al. [6] discovered high coupling factor of thickness vibration mode of  $k_{33}$  around 90% in PZNT single-crystal rod. The reason to obtain higher coupling factor due to domain alignments through DC poling illustrates in **Figure 2** from difference between single crystals (oriented domains) and ceramics (multidomains). In DC poling process, ferroelectric domains in single crystals become from multi-domains to oriented domains, and finally single (mono) domain in a crystal bulk, the dimensions of which more than several millimeter, while random-orientated ceramics become practical single domain in a ceramic grain, the dimensions of which around several microns. As the result, high coupling factors due to high domain alignment (high domain anisotropy) are realized in the crystal bulk without grain boundaries in comparison with oriented ceramic grains connected with each other by grain boundaries.

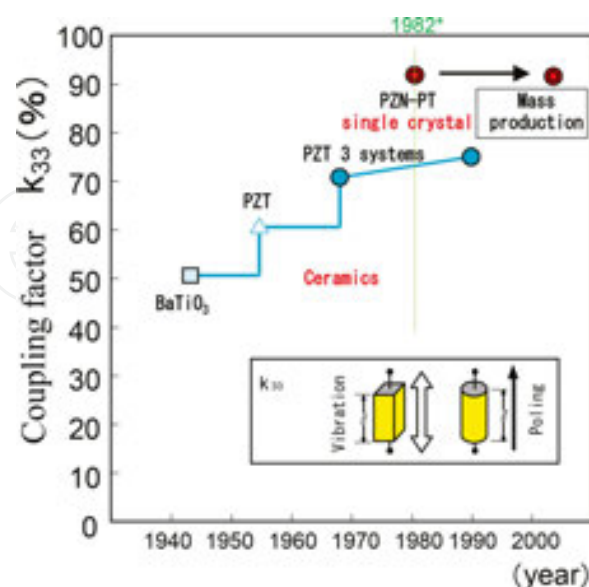


**Figure 1.** Improvement of electromechanical coupling factor on thickness vibration mode of  $k_{33}$  from piezoelectric ceramics to single crystals since 1942 discovered  $\text{BaTiO}_3$  [4].

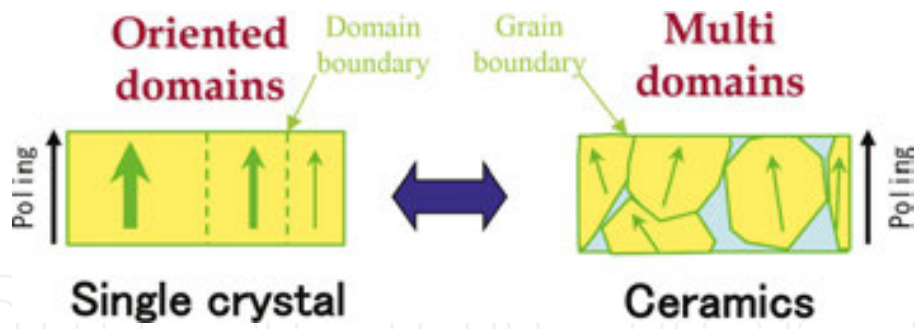


Figure 2. Difference in domain alignments between single crystals and ceramics.

### 1.3. High electromechanical coupling factor in relaxor single crystals

While relaxor single-crystal rods processed high coupling factor of  $k_{33}$  mode as mentioned previously, single-crystal plates were studied in cases of other vibration modes [7]. **Figure 3** shows single-crystal rod and plate composed of relaxor single crystal and the relationships between the dimensions and electromechanical coupling factors of  $k_{33}$  (thickness vibration mode),  $k_{31}$  (length vibration mode), and  $k_{32}$  (width vibration mode). The DC poling direction is the thickness direction of both the rod and the plate. In the case of the single-crystal plates, it can be expected higher domain alignment in the plates to obtain higher coupling factors of  $k_{31}$  and  $k_{32}$  modes. **Table 1** shows crystal plane dependence of coupling factors ( $k_{31}$ ,  $k_{32}$ ,  $k_{33}$ ), piezoelectric strain constants ( $d_{31}$ ,  $d_{33}$ ), remanent polarization ( $P_r$ ), coercive field ( $E_c$ ), and time aging for  $k_{31}$ , respectively. We discovered giant  $k_{31}$  over 80% and  $d_{31}$  over 1300 pC/N in (100)0.91Pb(Zn<sub>1/3</sub>Nb<sub>2/3</sub>)O<sub>3</sub>-0.09PbTiO<sub>3</sub> [(100)PZNT91/09] and (110)0.74Pb(Mg<sub>1/3</sub>Nb<sub>2/3</sub>)-0.26PbTiO<sub>3</sub> [(110)PMNT74/26] single-crystal plates [8]. The reason to obtain high  $k_{31}$  and  $d_{31}$  is due to achieve single (mono) domain alignment in the plates. Since PMNT compositions were preferred to produce single crystal in comparison with PZNT compositions because a pyrochlore phase is easily formed in PZNT together with perovskite phase, PMNT single crystal is

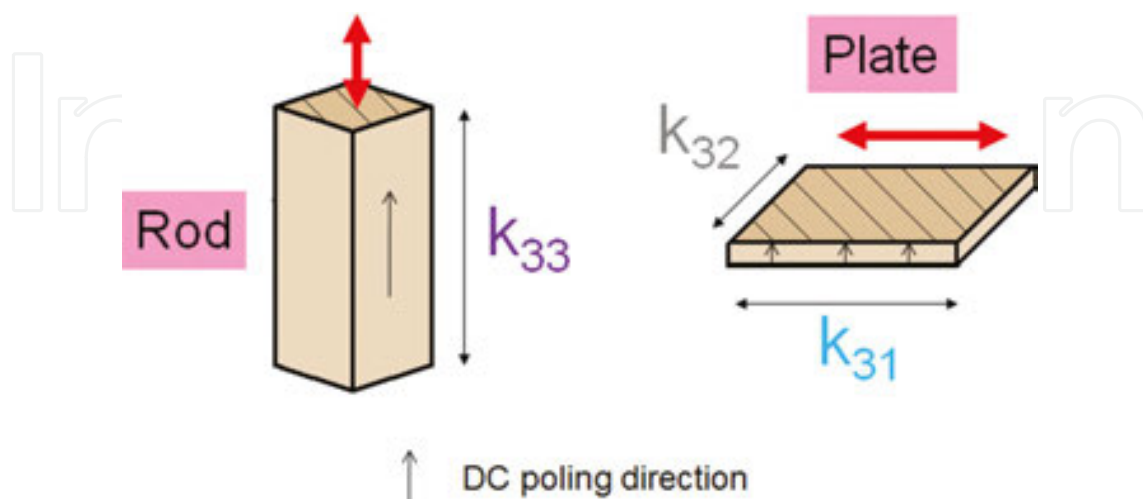


Figure 3. Vibration modes and coupling factors of single-crystal rod and plate in relaxor single crystal.

focused on to fabricate by flux Bridgman method [9]. While the quality of PMNT single crystal was improved through the mass production by trial and error, plate-shaped piezoelectric transducers for medical use were replaced PZT ceramic plate by PMNT single-crystal plate because of high  $k_t$  and high frequency of around 5 MHz (**Figure 4**) [5, 9].

Crystal plane	Single crystal	$k_{31}$ (%)	$-d_{31}$ (pC/N)	$k_t$ (%)	$d_{33}$ (pC/N)	$k_{32}$ (%)	Pr ( $\mu\text{C}/\text{cm}^2$ )	Ec (V/mm)	Aging
(100)	PZNT	86	2100	55	2400	42	35	600	Good
(100)	PMNT	65	1030	60	2420		22	300	NG
(110)	PZNT	30–60	300–720	40	530–1030				NG
(110)	PMNT	87	1320	48	970	69	30	200	
(111)	PZNT	20	~170	50	190–560				Good
(111)	PMNT				Small piezoelectricity				

**Table 1.** Crystal plane dependence of coupling factors ( $k_{31}$ ,  $k_t$ ,  $k_{32}$ ), piezoelectric strain constants ( $d_{31}$ ,  $d_{33}$ ), remanent polarization (Pr), coercive field (Ec), and time aging for  $k_{31}$  in PZNT and PMNT single-crystal plates.



**Figure 4.** Plate-shaped piezoelectric transducers utilizing relaxor single crystal for medical uses in cases of (a) and (b): abdominal (stomach etc.) use, and (c): circulatory organ (heart) use [5].

## 2. Characterization of relaxor single-crystal plates

### 2.1. Measurement of sound velocities in relaxor single-crystal plates

Sound velocities were measured in relaxor single-crystal plates (dimensions of 20.7 mm length, 14.0 mm width and 0.39 mm thickness) of (100)PMNT70/30 supplied by JFE Mineral Co., Ltd. using an ultrasonic precision thickness gauge (Olympus Model 35DL) with high-frequency (longitudinal wave: 30 and 20 MHz, and transverse wave: 20 and 5 MHz) pulse generation (**Figure 5**) [10, 11]. The measurement positions of Nos. ①–⑥ of sound velocities in the plate are shown in this figure. The directions of DC poling field and sound wave propagation are parallel to the thickness. The elastic constants in PMNT70/30 single-crystal plates calculated by the sound velocities were compared with the elastic constants in piezoelectric ceramic disks (dimensions of 14–20 mm diameter and 0.5–1.5 mm thickness) composed of PMNT70/30, PZT,

lead titanate, and lead free utilizing the equations as shown in **Figure 6** [11]. On the measurement of sound velocities in single-crystal plates, there are one longitudinal wave velocity ( $V_L$ ), and two transverse wave velocities ( $V_{S/L}$  and  $V_{S/W}$ ) in the directions of length and width in plate due to the anisotropy of the single-crystal plate (**Figure 7**) which are different from in the case of piezoelectric ceramics. However, the  $V_{S/W}$  is almost same as the  $V_{S/L}$  because of the same crystal anisotropy in the crystal plane of (100)PMNT70/30 as mentioned the following experimental results.

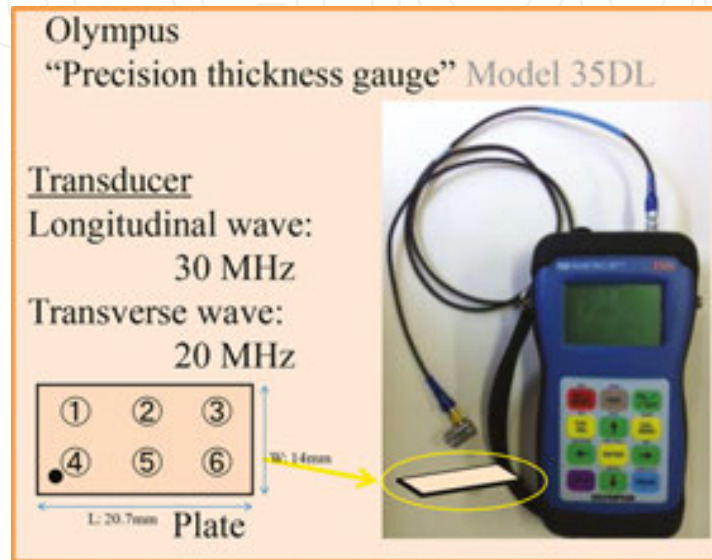


**Figure 5.** Equipment of sound velocity measurement and measurement positions of ①-⑥ in single-crystal plate.

Young's modulus Y (N/m <sup>2</sup> )	Poisson's ratio $\sigma$ (-)
$Y = 3\rho V_S^2 \frac{V_L^2 - \frac{4}{3}V_S^2}{V_L^2 - V_S^2}$	$\sigma = \frac{1}{2} \left\{ 1 - \frac{1}{\left(\frac{V_L}{V_S}\right)^2 - 1} \right\}$
Modulus of rigidity G (N/m <sup>2</sup> )	Bulk modulus K (N/m <sup>2</sup> )
$G = \rho V_S^2$	$K = \rho \left( V_L^2 - \frac{4}{3}V_S^2 \right)$

$\rho$  : Density (kg/m<sup>3</sup>),  $V_L$  : Longitudinal wave velocity (m/s),  
 $V_S$  : Transverse wave velocity (m/s)

**Figure 6.** Elastic constants calculated by sound velocities using the equations.

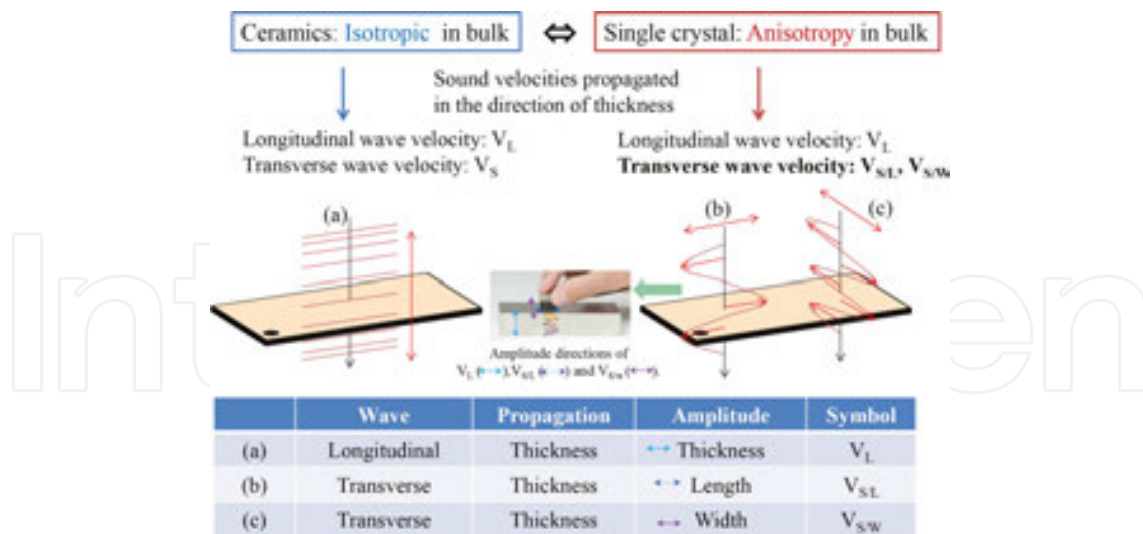


**Figure 7.** Propagation and amplitude directions of longitudinal and transverse waves in ceramics and single-crystal plate.

## 2.2. Piezoelectric and elastic constants

**Table 2** shows the dielectric and piezoelectric constants for six samples (Nos. 1–6) of PMNT70/30 single-crystal plates. Dielectric and piezoelectric constants were measured using an LCR meter (HP4263A), an impedance/gain phase analyzer (HP4194A) and a  $d_{33}$  meter (Academia Sinia: ZJ-3D). The piezoelectric strain constant  $d_{33}$  is an average value measured at six positions in the plate as mentioned previously. The  $d_{33}$  and relative dielectric constant ( $\epsilon_r$ ) are considerably high of 1710–1870 pC/N and 5810–6740 due to the high domain alignment in single-crystal plate. In addition,  $k_t$  is also rather high value of 63.1% suitable to a plate transducer with thickness mode.

Nos.	$d_{33}$ (pC/N)	$\epsilon_r$ (-)	$k_{31}$ (%)	$k_{32}$ (%)	$k_t$ (%)	$fc_{31}$ (Hz m)	$fc_{32}$ (Hz m)	$fc_t$ (Hz m)
1	1750	5888	30.5	74.5	63.3	736	838	2299
2	1712	5814	30.8	74.3	63.1	737	836	2293
3	1697	5796	30.1	74.3	63.1	743	837	2290
4	1810	6334	30.4	74.6	63.4	709	814	2291
5	1873	6569	27.6	69.0	62.6	700	823	2306
6	1837	6740	29.8	72.4	63.1	700	818	2293

**Table 2.** Dielectric and piezoelectric constants for six samples (Nos. 1–6) of PMNT70/30 single-crystal plates;  $fc_{31}$ ,  $fc_{32}$  and  $fc_t$  mean frequency constants (a half of sound velocities) in  $k_{31}$ ,  $k_{32}$  and  $k_t$  modes.

**Figure 8** shows  $V_L$ ,  $V_{S/L}$  and  $V_{S/W}$  at each measuring position of Nos. ①–⑥ in the plates (Nos. 1–6). The  $V_{S/L}$  is almost same as the  $V_{S/W}$  in all the plates of Nos. 1–6 because of the same crystal anisotropy of the crystal plane of (100)PMNT70/30. While the fluctuation [the difference in

maximum and minimum values ( $\Delta$ ) of  $V_L$ ,  $V_{S/L}$  and  $V_{S/W}$  in No. 2 is 3, 5, and 3 m/s, the fluctuation in No. 5 is considerably large values of  $\Delta V_L = 47$  m/s,  $\Delta V_{S/L} = 182$  m/s and  $V_{S/W} = 152$  m/s even though the  $k_t$ 's are almost same (**Table 2**). The fluctuation of  $V_L$ ,  $V_{S/L}$  and  $V_{S/W}$  in Nos. 5 and 6 corresponds to larger values of  $d_{33}$  and  $\epsilon_r$  in comparison with the ones in Nos. 1–4 (**Table 2**). Therefore, it was clarified that the measurement of sound velocities is effective tool to precisely evaluate local domain alignments in single-crystal plates.

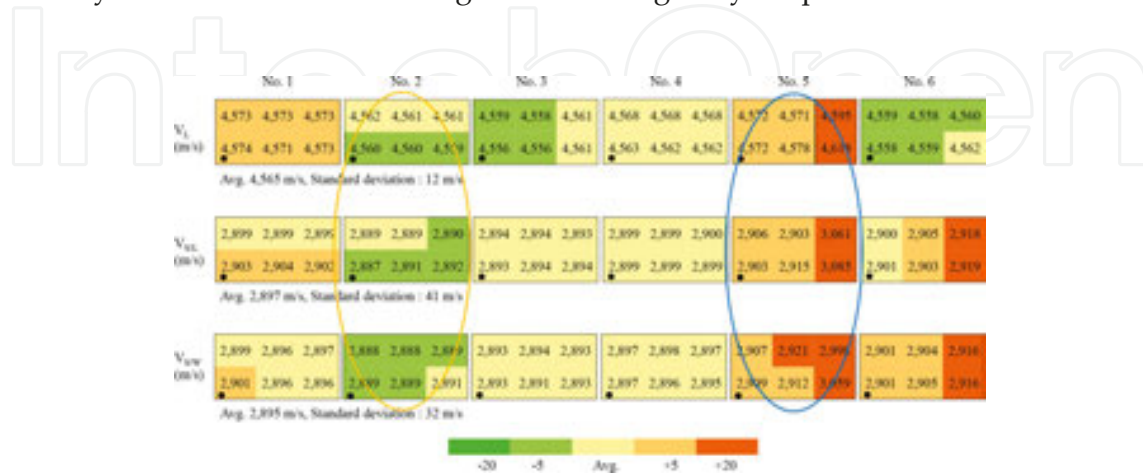


**Figure 8.** Distributions of longitudinal wave velocity ( $V_L$ ) and transverse wave velocities ( $V_{S/L}$  and  $V_{S/W}$ ) in PMNT70/30 single-crystal plates.

**Figures 9 and 10** show distributions of  $Y$  (in this case also  $Y_L = Y_W$ ) and  $\sigma$  ( $\sigma_L = \sigma_W$ ), and further,  $G$  ( $G_L = G_W$ ) and  $K$  ( $K_L = K_W$ ) in the plates of Nos. 1–6. Although the fluctuation of  $Y$ ,  $\sigma$ ,  $G$ , and  $K$  ( $\Delta Y$ ,  $\Delta \sigma$ ,  $\Delta G$  and  $\Delta K$ ) in Nos. 1–4 is much smaller than the  $\Delta Y$ ,  $\Delta \sigma$ ,  $\Delta G$ , and  $\Delta K$  in Nos. 5 and 6. **Figure 11** shows distributions of  $d_{33}$  in the plates of Nos. 1–6, the schematic domain alignments in the case of Nos. 2 and 5, and contribution of  $\epsilon_a$  ( $\epsilon_r$  of a-axis direction) and  $\epsilon_c$  ( $\epsilon_r$  of c-axis direction) to  $\epsilon_r$ . The reason higher  $d_{33}$  was obtained in the plates of Nos. 5 and 6 composed of oriented domain alignment is due to higher  $\epsilon_r$  affected by  $\epsilon_a$  ( $\epsilon_a > \epsilon_c$ ) under the



**Figure 9.** Distributions of Young's modulus ( $Y_L$  and  $Y_W$ ) and Poisson's ratio ( $\sigma_L$  and  $\sigma_W$ ) in PMNT70/30 single-crystal plates.

condition of same  $k_i$ 's. On the contrary, the plates of Nos. 1–4 consist of single domain alignment, the  $\epsilon_r$  of which practically depends on  $\epsilon_c$ . These domain configurations between the plates of Nos. 1–4 and Nos. 5, 6 will be described in the Sections 2.3–2.5.



Figure 10. Distributions of modulus of rigidity ( $G_L$  and  $G_W$ ) and bulk modulus ( $K_L$  and  $K_W$ ) in PMNT70/30 single-crystal plates.

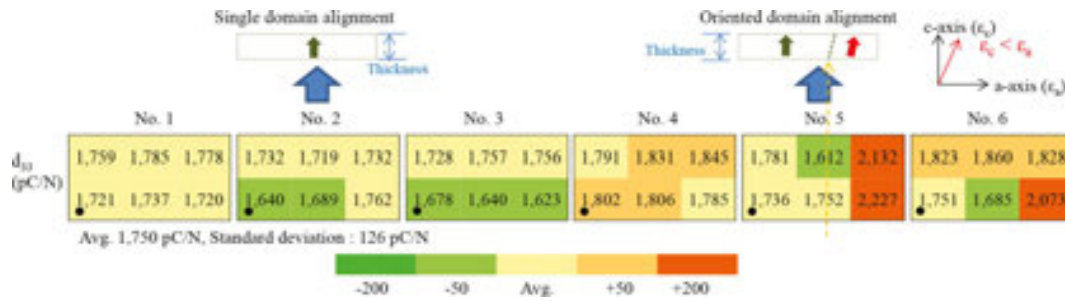


Figure 11. Distributions of  $d_{33}$  in the plates, the schematic domain alignments in the case of Nos. 2 and 5, and contribution of  $\epsilon_a$  ( $\epsilon_r$  of a-axis direction) and  $\epsilon_c$  ( $\epsilon_r$  of c-axis direction) to  $\epsilon_r$ .

### 2.3. Effect of domain boundaries on elastic constants

Figure 12 shows relationships between elastic constants ( $Y$ ,  $\sigma$ ,  $G$ , and  $K$ ) and  $d_{33}$  in the plates of Nos. 1–6. There are two groups such as single domain alignment (low  $Y$ ,  $G$  and high  $\sigma$ ,  $K$  of Nos. 1–4) and oriented domain alignment (high  $Y$ ,  $G$  and low  $\sigma$ ,  $K$  of Nos. 5 and 6). Comparing the two groups, while the domain configurations change from oriented domain alignment (plates of Nos. 5 and 6) to single domain alignment (plates of Nos. 1–4), the  $Y$  and  $G$  decrease, and  $\sigma$  and  $K$  increase. Here, the plates with oriented domain alignment mean the plates possess domain boundaries just like grain boundaries as mentioned later. It was thought that the existence of domain boundaries like grain boundaries acts as the increase in  $Y$ ,  $G$  and the decrease in  $\sigma$  and  $K$  as same as in the case of ceramics.

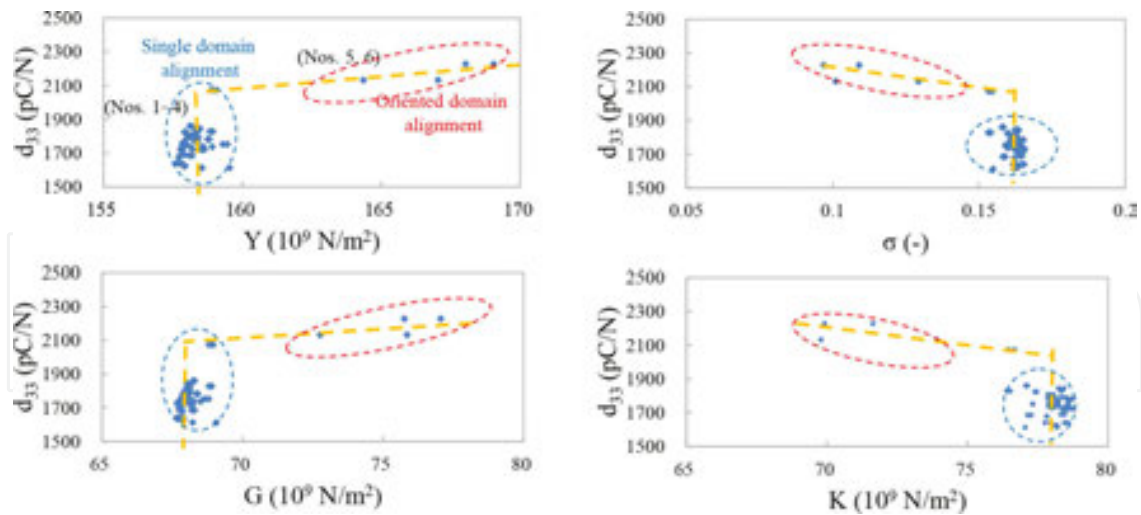


Figure 12. Relationships between elastic constants and  $d_{33}$  in plates.

#### 2.4. Frequency responses in single-crystal plates

Frequency responses of impedance in the plates were measured to investigate the vibration modes. There are  $k_t$  fundamental and the overtones of 3rd, 5th, and 7th without any spurious responses in range from 1 to 50 MHz (Figure 13). Calculating from the impedance responses of  $k_t$  fundamental, the average  $k_v$  and the standard deviation are 63.1% and  $\sigma = 0.25\%$  ( $n = 6$  pcs.).

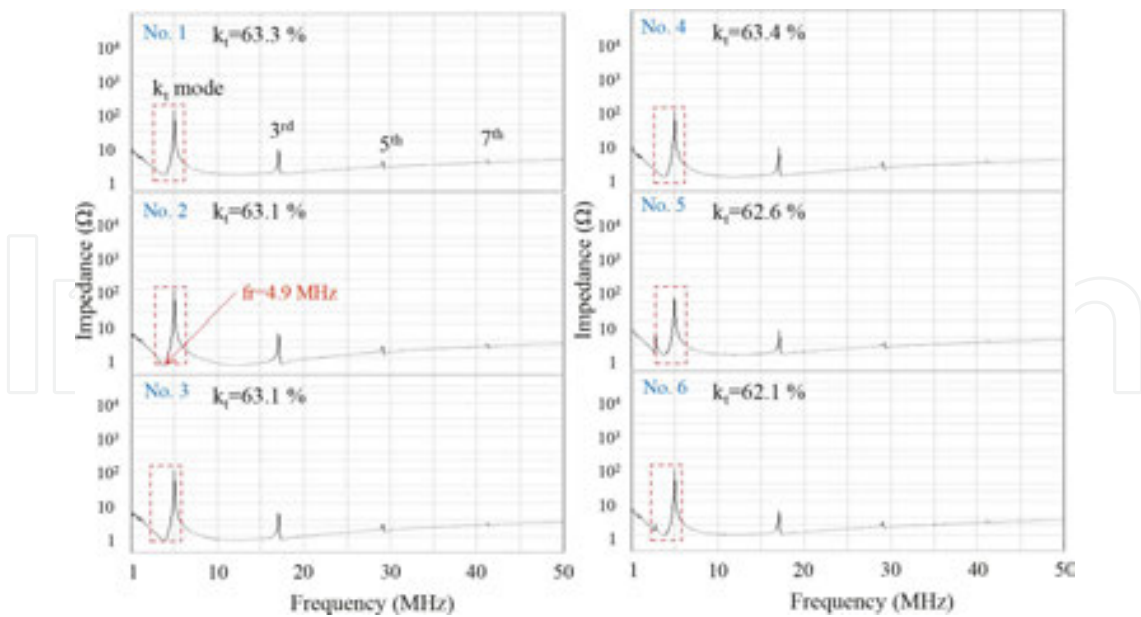


Figure 13. Frequency responses of impedance in single-crystal plates in range of from 1 to 50 MHz.

While frequency responses in range of 1–150 kHz were measured for analyzing  $k_{31}$  and  $k_{32}$  modes, there are simple responses in Nos. 1–4; however, there are complicated responses with

spurious responses in Nos. 5 and 6 (**Figure 14**). Since the complicated responses were related to  $k_{31}$ ,  $k_{32}$  modes and their overtones [12], it was evident that different domain configurations exist in the plates of Nos. 5 and 6 as well as the investigation on measuring sound velocities.

IntechOpen

**Figure 14.** Frequency responses of impedance in single-crystal plates in range of from 1 to 150 kHz.

## 2.5. Observation of ferroelectric domains by transmission optical microscope

Single-crystal plates removed electrodes for DC poling use, after DC poling and after depolarization at 200°C, were investigated by a transmission type optical microscope under cross nicol to directly observe the domain configurations. **Figure 15** shows photos of the plates of Nos. 2 and 5 after DC poling (a) and after depolarization (b), and schematic pictures of domain alignments of the plates (Nos. 2 and 5) after depolarization. Although the photo of No. 2(a) indicates uniform color, the photo of No. 5(a) consists of two different color regions after DC poling. As the subtle difference in colors indicates the difference in domain alignment of the crystal bulk itself [12], it is thought that the plate of No. 5(a) is composed of more than two kinds of domain configuration (oriented domain alignment, moreover, there are domain boundaries just like grain boundaries), and on the other hand, the plate of No. 2(a) becomes uniformity (single domain alignment). The observations of the plates of Nos. 2(b) and 5(b) after depolarization more clearly show these domain configurations as described in the schematic pictures. Comparing the photos of Nos. 5(a) and (b), it can be concluded that the domain alignments have already existed in as-grown single-crystal plate such as grain boundaries in ceramics (it means domain boundaries just like grain boundaries). It was thought that these boundaries come from some kinds of mechanical stress because single-crystal plates are quite uniform from the viewpoints the investigation of the chemical compositions and the physical properties analyzed by XRD in the plates [9].

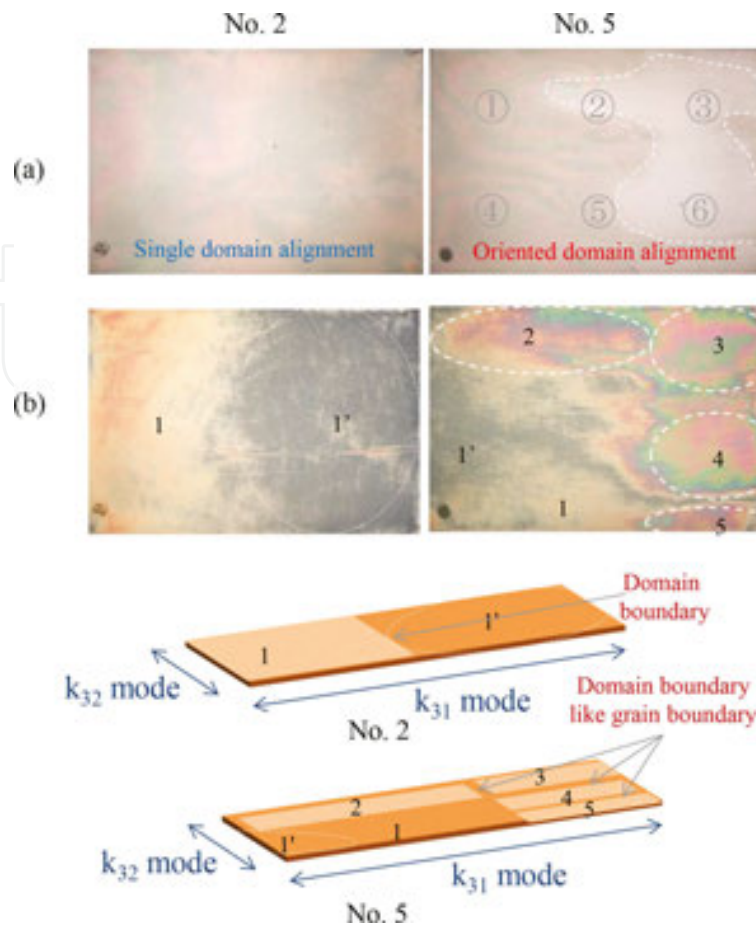


**Figure 15.** Observation of domain alignments in single-crystal plates by transmission optical microscope under cross nicol and schematic pictures of domain alignments of plates. Nos. ①–⑥ in this figure [No. 5(a)] correspond to measurement positions of sound velocities.

### 3. Elastic constant of PMNT70/30 single-crystal plates and ceramics

PMNT70/30 ceramics were fabricated to compare the two bodies, single-crystal plates, and ceramics. Evaluating elastic constants calculated by sound velocities, it was thought that effects of domain and grain boundaries on elastic constants can be clarified in both the cases.

#### 3.1. Piezoelectric properties and elastic constant in PMNT70/30 single-crystal plates and ceramics

**Table 3** shows dielectric and piezoelectric properties in PMNT70/30 single-crystal plates and ceramics. PMNT ceramics possessed the properties as follows: one-quarter of  $d_{33}$ , a half of  $\epsilon_r$  and two-third of  $k_t$  in comparison with the values of PMNT single-crystal plates. **Table 4** shows elastic constants in PMNT70/30 single-crystal plates and ceramics after DC poling. PMNT single-crystal plates possessed the properties as follows: almost same  $V_L$ , however, extremely

large  $V_s$  (+1000 m/s), as the result, small  $\sigma$  in comparison with the  $\sigma$  of PMNT ceramics. It is thought that the differences in the both are due mainly to grain boundaries as discussing later.

Single crystal	$d_{33}$ (pC/N)	$\epsilon_r$ (-)	$k_{31}$ (%)	$k_{32}$ (%)	$k_t$ (%)	$fc_{31}$ (Hz m)	$fc_{32}$ (Hz m)	$fc_t$ (Hz m)
Av.	1780	6190	29.9	73.2	63.1	721	828	2295
$\sigma$	65	377	1.1	2.0	0.3	18	10	6

PMNT70/30 single-crystal plate (dimensions; 20.7 mm<sup>L</sup>, 14.0 mm<sup>W</sup>, 1.00 mm<sup>T</sup>), n = 6 pcs.

**Table 3.** Dielectric and piezoelectric properties in PMNT70/30 single-crystal plates and ceramics after DC poling.

Ceramics	$d_{33}$ (pC/N)	$\epsilon_r$ (-)	$k_p$ (%)	$k_{31}^*$ (%)	$k_{32}^*$ (%)	$k_t$ (%)	$fc_p$ (Hz m)	$fc_{31}^*$ (Hz m)	$fc_{32}^*$ (Hz m)	$fc_t$ (Hz m)
Av.	420	3045	50.6	20.9	41.6	41.9	2167	1554	1703	2227
$\sigma$	7.5	60	1.0	-	-	0.5	7.7	-	-	4.4

PMNT70/30 ceramic disk (dimensions; 20.0 mm <sup>$\phi$</sup> , 1.00 mm<sup>T</sup>), n = 10 pcs.

\* PMNT70/30 ceramic plate (dimensions; 15.6 mm<sup>L</sup>, 10.9 mm<sup>W</sup>, 1.00 mm<sup>T</sup>), n = 1 pc.

PMNT70/30 manufacturing processes; Firing: 1200°C, 2h/ DC poling: 2 kV/mm, 30 min at RT.

**Table 3.** Continued.

Material	Elastic constants	Density (g/cm <sup>3</sup> )	$V_L$ (m/s)	$V_{s/L}$ (m/s)	$V_{s/W}$ (m/s)	$Y_L, Y_W$ ( $\times 10^{10}$ N/m <sup>2</sup> )
Single crystal	Av.	8.10	4565	2897	2895	15.8, 15.8
	$\sigma$	0.01	12	41	32	0.2, 0.2
Ceramics	Av.	7.89	4466		1862	7.61
	$\sigma$	0.02	12		12	0.09

**Table 4.** Elastic constants in PMNT70/30 single-crystal plates and ceramics after DC poling.

Material	Elastic constants	$\sigma_L, \sigma_{W(-)}$	$G_L, G_W$ ( $\times 10^{10}$ N/m <sup>2</sup> )	$K_L, K_W$ ( $\times 10^{10}$ N/m <sup>2</sup> )
Single crystal	Av.	0.16, 0.16	6.80, 6.79	7.82, 7.82
	$\sigma$	0.01, 0.01	0.19, 0.15	0.19, 0.14
Ceramics	Av.	0.395	2.73	12.1
	$\sigma$	0.002	0.03	0.01

**Table 4.** Continued.

### 3.2. Effect of DC poling and grain boundaries on elastic constants

**Figure 16** shows the effect of DC poling on elastic constants in PMNT70/30 single-crystal plates; elastic constants vs.  $d_{33}$  after DC poling and after depolarizing together with lead-containing

(PMNT, soft and hard PZT, lead titanate and PMNT) and lead-free (barium titanate, alkali niobate, and alkali bismuth titanate) ceramics. PMNT70/30 single-crystal plates after DC poling become mechanical hard because  $Y$ ,  $G$ ,  $\sigma$ , and  $K$  increase, while  $Y$  and  $G$  decrease and  $\sigma$  and  $K$  increase all kinds of ceramics [see the directions of each arrow ( $\rightarrow$ )]. It was thought since single crystal was improved mechanical hardness after DC poling, domain boundaries in PMNT70/30 single-crystal plate act as to absorb mechanical stress (generated by defects due to the boundaries).

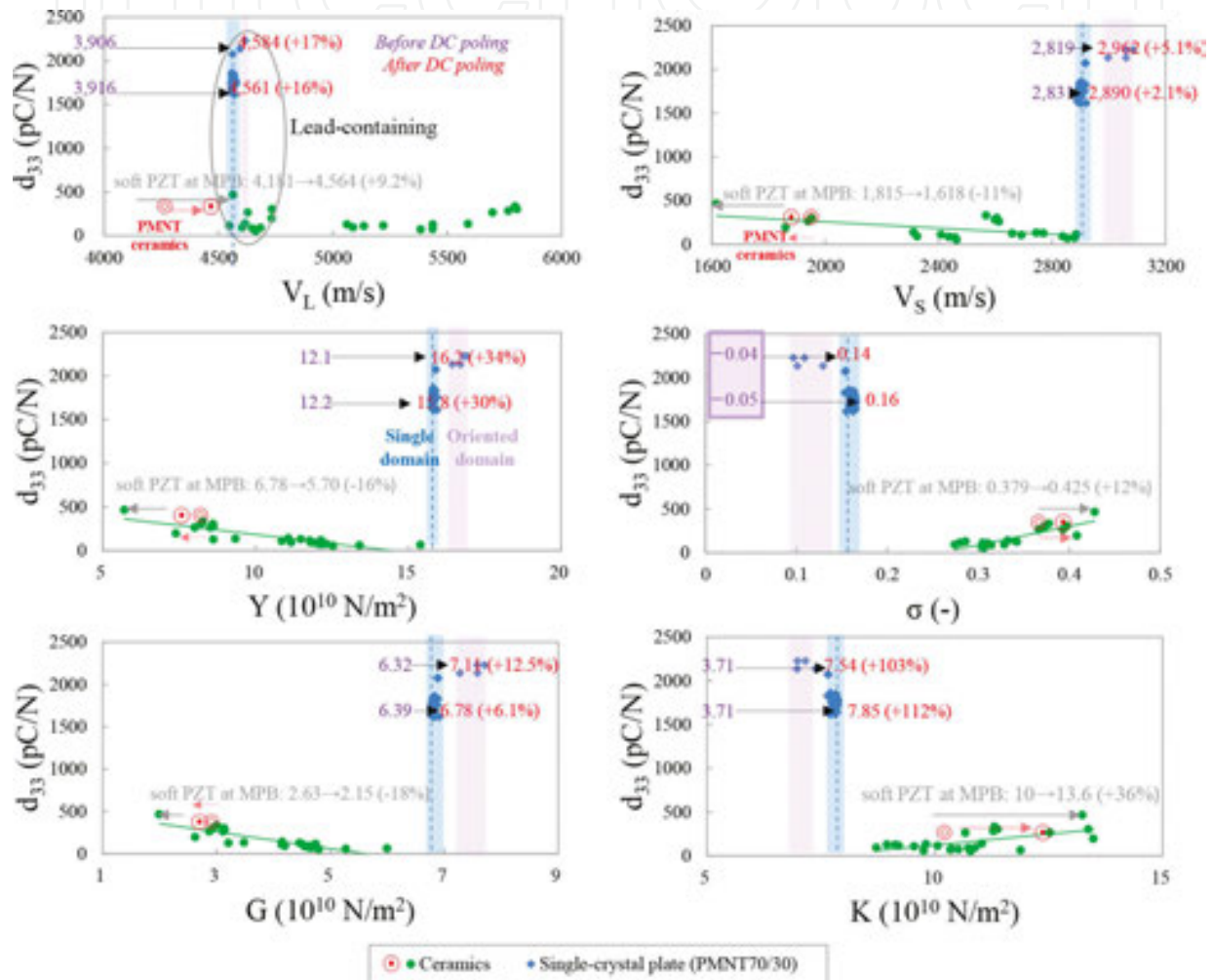


Figure 16. Effect of DC poling on elastic constants in PMNT70/30 single-crystal plates.

Figure 17 shows the effect of grain boundary between PMNT single-crystal plates and PMNT ceramics; elastic constants vs. various kinds of coupling factors ( $k$ ) such as  $k_p$  (planer coupling factor in ceramic disk),  $k_{31}$ ,  $k_{32}$ , and  $k_t$  in the single-crystal plates. Introducing grain boundary, in PMNT ceramics  $Y$  and  $G$  become smaller and  $\sigma$  and  $K$  become larger in comparison with the ones in single crystal [see the directions of each arrow ( $\rightarrow$ )]. Grain boundaries also act as to absorb mechanical stress by the defects due to the boundaries. Furthermore, increasing  $k$  ( $k_{31}$ ,  $k_{32}$ , and  $k_t$ ) in single crystal,  $Y$  and  $G$  decrease, and  $\sigma$  and  $K$  increase as same as the ones

of piezoelectric ceramics. It was thought that these counter phenomena ( $Y$  and  $G$  decrease, and  $\sigma$  and  $K$  increase) for increasing  $k$  between PMNT single-crystal plates and PMNT ceramics are due to domain alignment by DC poling field [11].

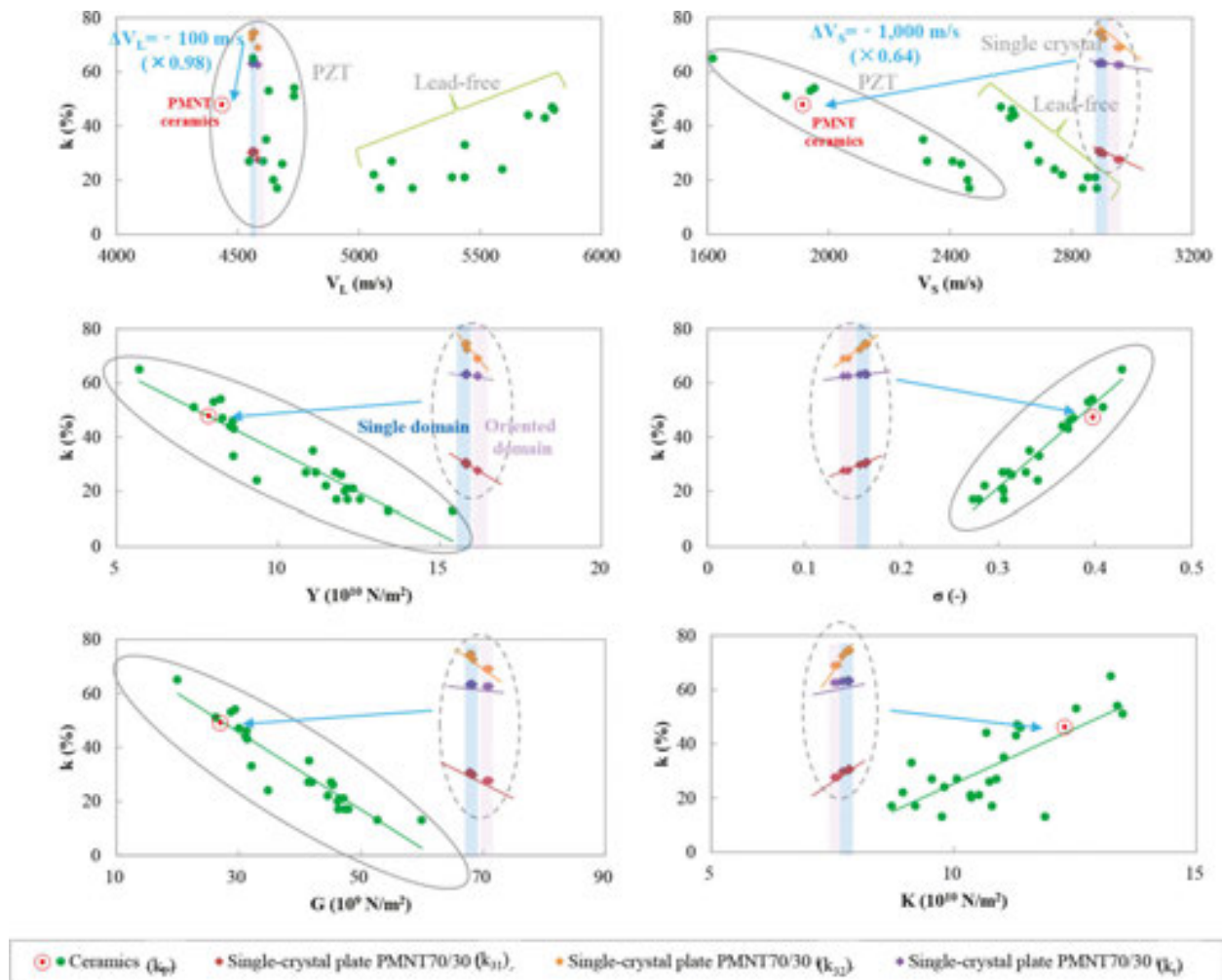
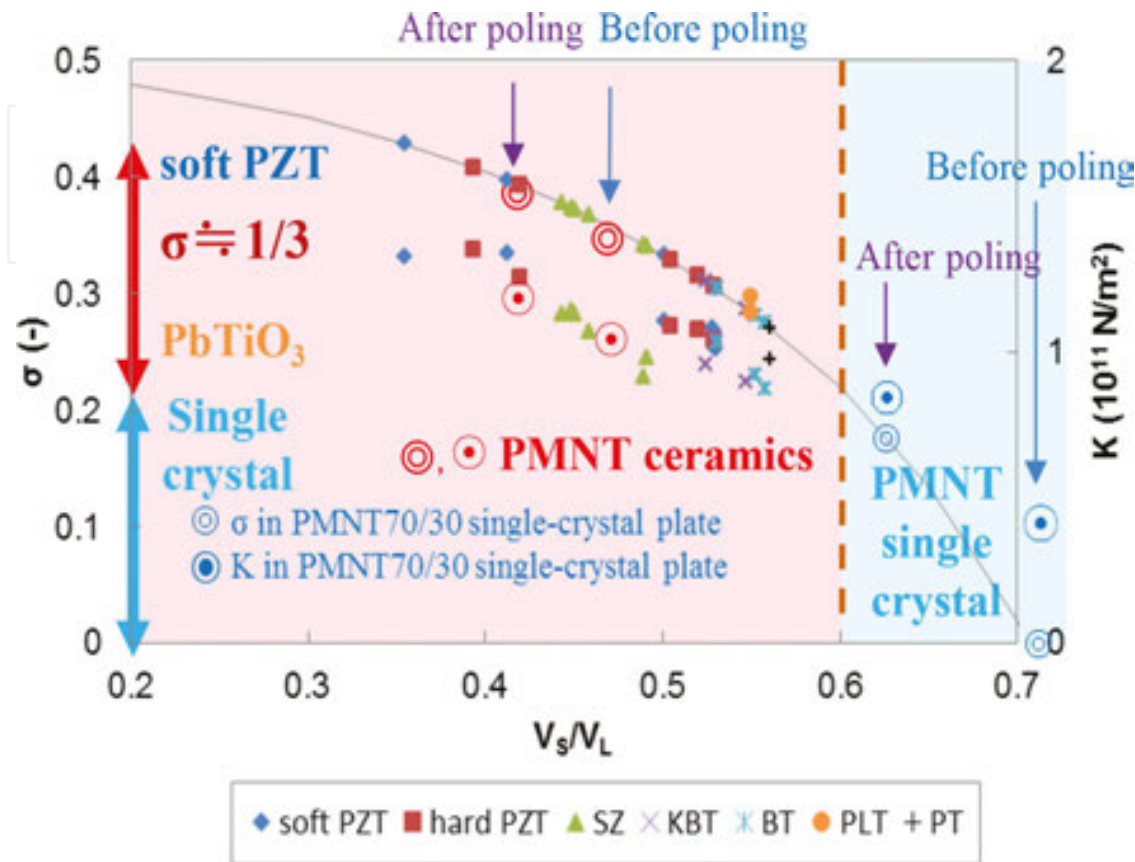


Figure 17. Effect of grain boundary between PMNT70/30 single-crystal plates and ceramics.

### 3.3. Relationships between sound velocities, Poisson’s ratio, and bulk modulus

Figure 18 shows the relationships between ratio of  $V_S$  to  $V_L$ ;  $V_S/V_L$ ,  $\sigma$ , and  $K$  in PMNT single-crystal plates and piezoelectric ceramics including PMNT ceramics. Since decreasing  $V_S/V_L$  increasing coupling factor ( $k$ ) from a result of our previous study [11],  $k$  increases with increasing  $\sigma$  and  $K$  in both the cases of single crystal and ceramic. However, the  $\sigma$  and  $K$  in single crystal are extremely small in comparison with the ones in ceramics; especially the  $\sigma$  in single crystal after depolarizing is zero. While the  $\sigma$  in ceramics distributes from 0.38 to 0.43 (soft PZT), from 0.36 to 0.40 (PMNT), and from 0.22 to 0.27 ( $PbTiO_3$ ), the  $\sigma$  in PMNT single crystal distribute from 0.0 to 0.16 before and after DC poling, respectively. The reason  $\sigma$ 's

become smaller from PZT, PMNT,  $\text{PbTiO}_3$  ceramics to PMNT single crystal depends on degree of the crystal anisotropy of the materials as shown in the ranges of  $\sigma$  (the longitudinal axis).



**Figure 18.** Relationships between ratio of  $V_s$  to  $V_L$ ;  $V_s/V_L$ ,  $\sigma$  and  $K$  in PMNT70/30 single-crystal plates and piezoelectric ceramics including PMNT70/30 ceramics.

#### 4. Origin of piezoelectricity in single-crystal plates and ceramics

From the viewpoints of elastic constants in single crystal and ceramics, the origin of piezoelectricity of both was proposed from viewpoints of elastic constants. In single crystal, low  $K$  accompanied with high  $Y$  and  $G$  and low  $\sigma$  is significant to realize high  $k$  because single crystal exhibits one grain (no grain boundary) with single domain (**Figure 17**). On the contrary, in ceramics high  $\sigma$  caused by high  $K$  accompanied with low  $Y$  and  $G$  is significant to realize high  $k$  because same charges introduced by domain alignment in each grain repulse each other after DC poling [11]. The repulsion of oriented domains in grains acts as increasing  $\sigma$  with increasing  $K$  and decreasing  $Y$  and  $G$ , as the results, high  $k$  can be achieve in ceramics with multi grains (practical single domain in one grain). Therefore, the origin of piezoelectricity in ceramics is said that the existence of grain boundaries; furthermore, the grain orientation accompanied with domain alignment between ceramic grains is the key. **Figure 19** is summarized the relationships between domain alignment, size dimensions, origin of piezoelectricity, and effect

of DC poling on elastic constants in single crystal and ceramics through our investigation of the measurement on sound velocities. From this figure, it is clearly understand between single and oriented domains in single crystal, and the relationships between size dimensions, domain and grain alignments, and the effect of DC poling on elastic constants in piezoelectric materials.

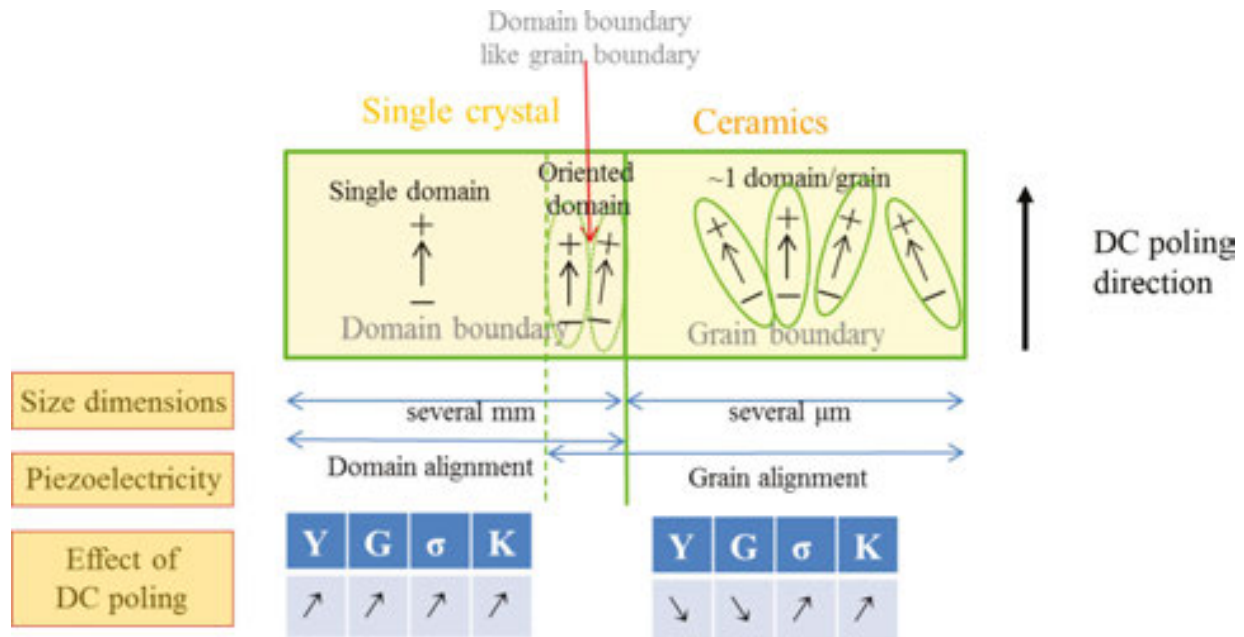


**Figure 19.** Relationships between domain alignment, size dimensions, piezoelectricity, and effect of DC poling on elastic constants in single crystal and ceramics.

## 5. Summary

Roles of domain and grain boundaries in relaxor single-crystal plates and ceramics were clarified by measuring sound velocities. Effect of domain boundaries on elastic constants was evaluated by the effect of DC poling on elastic constants in  $(100)0.70\text{Pb}(\text{Mg}_{1/3}\text{Nb}_{2/3})\text{O}_3-0.30\text{PbTiO}_3$  relaxor single-crystal plates. Effect of grain boundary on elastic constants was evaluated by comparing elastic constant in the relaxor single crystals and the ceramics. Finally, the different origins of piezoelectricity in single crystals and ceramics were proposed through our investigation of the measurement on sound velocities.

## Acknowledgements

This work was partially supported by two Grants-in-Aid for Scientific Research C (Nos. 21560340 and 26420282), a Grant from the Strategic Research Foundation Grant-Aided Project for Private Universities 2010–2014 (No. S1001032) from the Ministry of Education, Culture,

Sports, Science and Technology, Japan (MEXT), and a Cooperation Research Foundation 2014–2015 between Academy and Industry of Fukuroi City, Shizuoka, Japan.

## Author details

Toshio Ogawa

Address all correspondence to: [ogawa@ee.sist.ac.jp](mailto:ogawa@ee.sist.ac.jp)

Department of Electrical and Electronic Engineering, Shizuoka Institute of Science and Technology, Fukuroi, Shizuoka, Japan

## References

- [1] Cross LE. Relaxor ferroelectrics. *Ferroelectrics* 1987;76:241–267.
- [2] Yamashita Y, Harada K, Saitoh S. Recent applications of relaxor materials. *Ferroelectrics* 1998;219:29–36.
- [3] Jaffe B, Cook WR, Jaffe H. *Piezoelectric ceramics*. London: Academic Press; 1971.
- [4] Wainer E, Salomon N. Electrical reports titanium alloys manufacturing division. National Lead Co. Reports. 1938–1943;8–10.
- [5] Yamashita Y. Study on lead scandium niobate piezoelectric ceramics. Doctor dissertation of Waseda University. 1998 (in Japanese).
- [6] Kuwata J, et al. Dielectric and piezoelectric properties of  $0.91\text{Pb}(\text{Zn}_{1/3}\text{Nb}_{2/3})\text{O}_3$ – $0.09\text{PbTiO}_3$  single crystals. *Japanese Journal of Applied Physics* 1982;21:1298–1303.
- [7] Ogawa T, et al. Giant electromechanical coupling factor of  $k_{31}$  mode and piezoelectric  $d_{31}$  constant in  $\text{Pb}[(\text{Zn}_{1/3}\text{Nb}_{2/3})_{0.91}\text{Ti}_{0.09}]\text{O}_3$  piezoelectric single crystal. *Japanese Journal of Applied Physics* 2002;41:L55–L57.
- [8] Ogawa T. Giant  $k_{31}$  relaxor single-crystal plate and their applications. In: Lallart M. ed. *Ferroelectrics—Applications*. Rijeka: InTech; 2011, 3–34.
- [9] Matsushita M, et al. Abstract of the American Ceramic Society. 103rd Annual Meet. 2001:247.
- [10] Ogawa T. Acoustic wave velocity measurement on piezoelectric ceramics. In: Ebrahimi F. ed. *Piezoelectric materials and devices—Practice and applications*. Rijeka: InTech; 2013, 35–55.

- [11] Ogawa T. Origin of piezoelectricity in piezoelectric ceramics from viewpoints of elastic constants measured by acoustic wave velocities. In: Barranco AP. ed. *Ferroelectric materials—Synthesis and characterization*. Rijeka: InTech; 2015, 33–58.
- [12] Ogawa T, Numamoto Y. Origin of giant electromechanical coupling factor of  $k_{31}$  mode and piezoelectric  $d_{31}$  constant in  $\text{Pb}[(\text{Zn}_{1/3}\text{Nb}_{2/3})_{0.91}\text{Ti}_{0.09}]\text{O}_3$  piezoelectric single crystal. *Japanese Journal of Applied Physics*. 2002;41:7108–7112.

IntechOpen

IntechOpen